Martian Cirrus-like Hazes at the Phoenix Landing Site. M. T. Lemmon, Texas A&M University, 3150 TAMU, College Station, TX, lemmon@tamu.edu

Introduction: Water vapor in the Martian atmosphere condenses into ice hazes and clouds [1]. The ice particles have been considered to be of the few micron scale, within a factor of two of the dust size [2]. Phoenix lidar measurements during the Arctic summer showed nighttime and early morning condensation into low cloud layers, with morphologies that suggested ice particle radii near 30 microns [3]. Solar imaging by the Phoenix Surface Stereo imager (SSI) provides a mission-long record of dust optical depth, showing ice-haze events late in the mission. Such ice-haze events allow a diffraction-based estimate of ice particle sizes, which tend to be 20-40 micron radius. Further, SSI observations give a coarse grained look at changes in the water vapor column, which are not correlated with observable cloud events and suggest another mechanism, such as adsorption into soil, is responsible for depleting atmospheric water.

Discussion: The Phoenix mission operated over 152 sols (Martian days of about 24h39m each) during 2008, from solar longitude 77° to 149° (where 0° is northern spring equinox and 90° is northern summer solstice) at a latitude of 68° N. The SSI documented the landscape and atmosphere throughout that period. Surface imaging showed frequent frost in trenches late in the mission, but few events of frost formation in undisturbed terrain [4]. Images of the Sun were taken in several filters, at many times, on nearly all sols. Those images show increasing solar attenuation as the Sun gets lower in the sky, allowing a relative calibration similar to that done for other missions [5-7].

Optical depths from sols 40 to 151 (Fig. 1) show a decline in the overall value, followed by increasing events of sub-sol duration (later identified as typically ice) and multi-sol duration (dust storms). Short-duration spikes were generally seen during the 0100-0600 local true solar time (LTST) interval, during which ice clouds have been identified by lidar [3].

In addition, each of those spikes and several other data show a distinctive appearance. An example sunrise image (Fig. 2) shows the disk of the Sun set against a twilight sky and bisect by the horizon. Unlike typical Mars Exploration Rover (MER) images of sunsets, this image shows a bright aureole immediately around the Sun, with an exponential brightness fall off having a ~0.5° scale, which is also bisected. The typical scale for brightness decay near the Sun for dust is ~4-12° [8]. This suggests a population of large particles with a more narrow diffraction peak than dust.

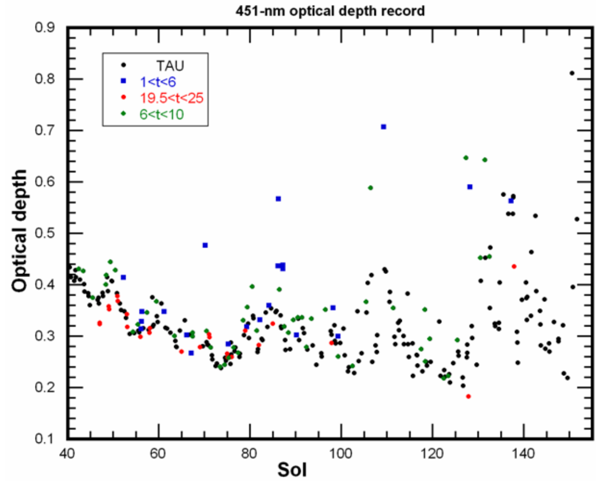

Figure 1. Blue filter optical depths are shown for the Phoenix mid- to late-mission. Shown are individual records from 1000-1930 local true solar time (black), 1930-0100 (red), and 0100-0600 (blue). There are no significant differences in other wavelengths.

Figure 2. The Sun was imaged rising on the morning of sol 90. Atmospheric scattered light is seen around the Sun and blocked by the horizon.

A similar effect can be seen in a minority of solar filter images of the Sun when it is higher in the sky, Figure 3 shows 2 representative images, one showing a similar narrow aureole, and one showing a more typical Sun image that is also similar to MER and Pathfinder Sun images [6,7]. The brightness fall off is consistent with diffraction by 20-50 micron particles (time-varying) present at optical depths from hundredths to tenths. Optical depths of tenths or more are equivalent to a few precipitable microns, and are confined to 0100-1000 LTST except for one observation at noon on sol 150. Detectable ice with optical depths less than tenths only occur 3 times from 1600-0100, and do not occur after 1000 until sol 130, but are common for 0100-1000. These times are broadly consistent with lidar results [3]

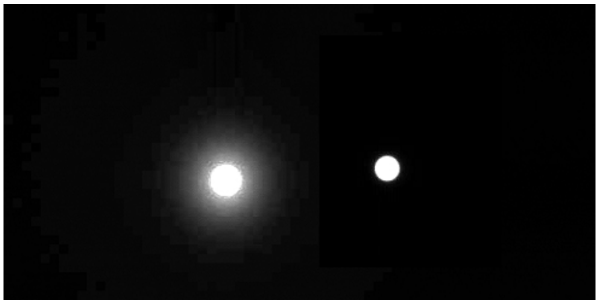

Figure 3. Two blue solar-filter images show the Sun during icy (left) and non-icy conditions (right). Contrast is stretched the same in each image.

The SSI also has 2 filters sensitive to the weak 935-micron water vapor absorption. About 35-40 precipitable microns of water vapor were seen during the day from sol 30 to 100, with a fall-off as the atmosphere cooled late in the mission (Fig. 4). Optical depths from 2130-0330 were typically near 20 precipitable microns over the interval such observations were taken. The column abundance of water in the clouds (few microns) is small compared to the error bars, but the diurnal variation is statistically significant.

Figure 5 shows the average diurnal profile. Note that the time when water vapor leaves the atmosphere does not correspond to a cloudy time frame as indicated above. Adding 15±5 microns of water to clouds would require a cloud optical depth of several tenths for 35 micron particles, and of 10 for 1.5 micron particles. Thus it appears that the water vapor that systematically leaves the atmosphere over 2000-2300 LTST does not go into haze. It also does not go into frost, which was rare despite frequent observations in the early morning hours. Thus it is likely the water is adsorbed into the soil. This is consistent with soil properties observations, and with a large swing in relative humidity near the surface that suggests vapor removal is confined to the bottom km or so of the atmosphere [9].

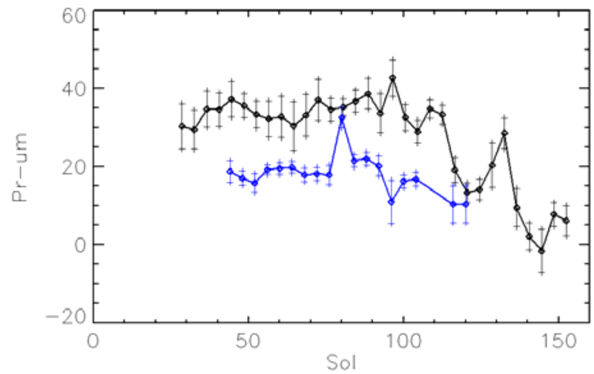

Figure 4. Water vapor column abundance in precipitable microns. Daytime values (black, 0530-1830) and “nighttime” values (blue) are shown. The latter are defined as data from 2130-0330, even though the Sun is up and imaged for the measurement.

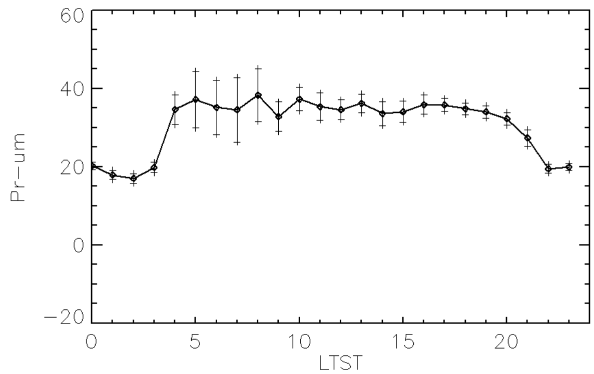

Figure 5. Water vapor column abundance through the sol (local true solar time) is shown in precipitable microns. All data from prior to sol 110 are averaged in bins of ±1 hour.

References: [1]Kahn, R. (1990). *J.Geophys.Res*. **95**, 14677-14693. [2]Clancy, R.T., *et al.* (2003). *J.Geophys.Res*. **108**, E9, 5098. [3] J.A. Whiteway, *et al.*. (2009). *Science* **325**, 68-70. [4] Smith, P.H.., *et al.* (2009) *Science* **325**, 58-61.. [5] Colburn, D.S., *et al.* (1989). *Icarus* **79**, 159-189. [6] Smith, P.H. and M.T. Lemmon (1999). *J.Geophys.Res*. **104**, 8975-8985. .[7] Lemmon, M.T., *et al.* (2004). *Science* **306**, 1753-1756. [8] Tomasko, M.G., *et al.* (1999). *J.Geophys.Res*. **104**, 8987-9007. . [9] Tamppari *et al.* (2009). *J. Geophys. Res.*, in press. doi: 10.1029/ 2009JE003415.